

05,08

Critical indices of magnetic phase transitions as indicators of the topology of exchange interaction in holmium films

© R.B. Morgunov^{1,2,3} S.N. Kashin¹, R.A. Valeev³, V.P. Piskorskii³, M.V. Burkanov³

¹Federal Research Center of Problems of Chemical Physics and Medicinal Chemistry RAS, Chernogolovka, Russia

²Tambov State Technical University, Tambov, Russia

³All-Russian Scientific Research Institute of Aviation Materials of the Research Center „Kurchatov Institute“, Moscow, Russia

E-mail: spintronics2022@yandex.ru

Received April 26, 2024

Revised April 26, 2024

Accepted April 30, 2024

Transitions between different types of spin ordering in holmium films have been studied in the temperature range 10–140 K and magnetic fields 0–4 T. The magnetic phase diagram in H – T coordinates indicates the presence of transitions between intermediate helicoid phases from the helix state to such spin structures, such as ferromagnet (ferro), fan (fan) and sliding structures (spin-slip). Arrott’s method made it possible to determine the critical indices for each of the transitions. Based on the critical indices, a selection of models and their combinations applicable to describe the mentioned non-collinear spin states was made.

Keywords: holmium films, spin structures, spin-reorientation transition, critical indices.

DOI: 10.61011/PSS.2024.05.58499.106

1. Introduction

Holmium demonstrates various types of spin ordering below the Curie temperature. Besides the collinear ferromagnetic state, various magnetic phases (fan, helix, spin-slip) existing below the Néel temperature 133 K are observed (Figure 1). These spin structures are formed as a result of exchange interaction competition with magnetic anisotropy and of the contact exchange interaction difference in and between the layers of the hexagonal lattice of holmium. In particular, the exchange interaction ratio between the adjacent layers and next neighbors is important [1]. All these factors depend on temperature that results in switching the spin structure when it changes. Increase in the magnetic field and corresponding Zeeman energy changes the energy balance of exchange interactions and magnetic anisotropy also resulting in switching between various spin configurations.

In [2], we established the boundaries of transitions between the abovementioned states in 400 nm holmium films (Figure 2). The phase diagram in the field H — temperature — T coordinates for holmium films has no significant difference from the phase diagrams established by other authors for bulk holmium samples [3,4]. This is due to the fact that the thickness of the 400 nm film is much higher than the maximum known period of spin structures in holmium ~ 30 – 40 nm [5]. For example, the period of rotation of spin helix in the helicoidal spin structure is equal to 12 constants of 5.6 Å lattice along the crystallographic axis c .

Magnetic phase transitions between various states may be characterized by critical indices determined from the

Arrott plot [6]. Though the spin configuration analysis and Arrott method are based on the Weiss molecular-field theory that assumes proportion between the ferromagnetic self-magnetic field and magnetization, this method may be used even when the Weiss theory is not applicable. Magnetic phase transition analysis is based on the Arrott–Noakes equation that correlates magnetization M and magnetic field H [6]:

$$(H/M)^{1/\gamma} = \frac{(T - T_c)}{T_c} + \left(\frac{M}{M_0}\right)^{1/\beta}, \quad (1)$$

where γ and β are critical parameters to be determined and compared with their values for known exchange interaction models. For example, critical parameters in the mean-field model are equal to $\beta = 0.5$, $\gamma = 1.0$ and are determined from $M(H)$ that will be a straight line in $M^2(H/M)$ coordinates. Positive slope of the straight line in $M^2(H/M)$ coordinates indicates a second-order transition, while a negative slope corresponds to a first-order transition. Theoretical coefficients known from literature for various exchange interaction models [7–9] are listed in Table 1.

Mean-field, Ising, Heisenberg and tricritical models listed in Table 1 differ in the exchange interaction contribution for x , y , z spin components and define the topology of ordered spin configuration that may be two-dimensional (2D Ising model) or three-dimensional (Heisenberg model) in the limiting cases. Of course, universality classes in Table 1 and the corresponding critical indices not necessarily occur in particular spin system. Mixed situations with intermediate values of β , γ are often observed.

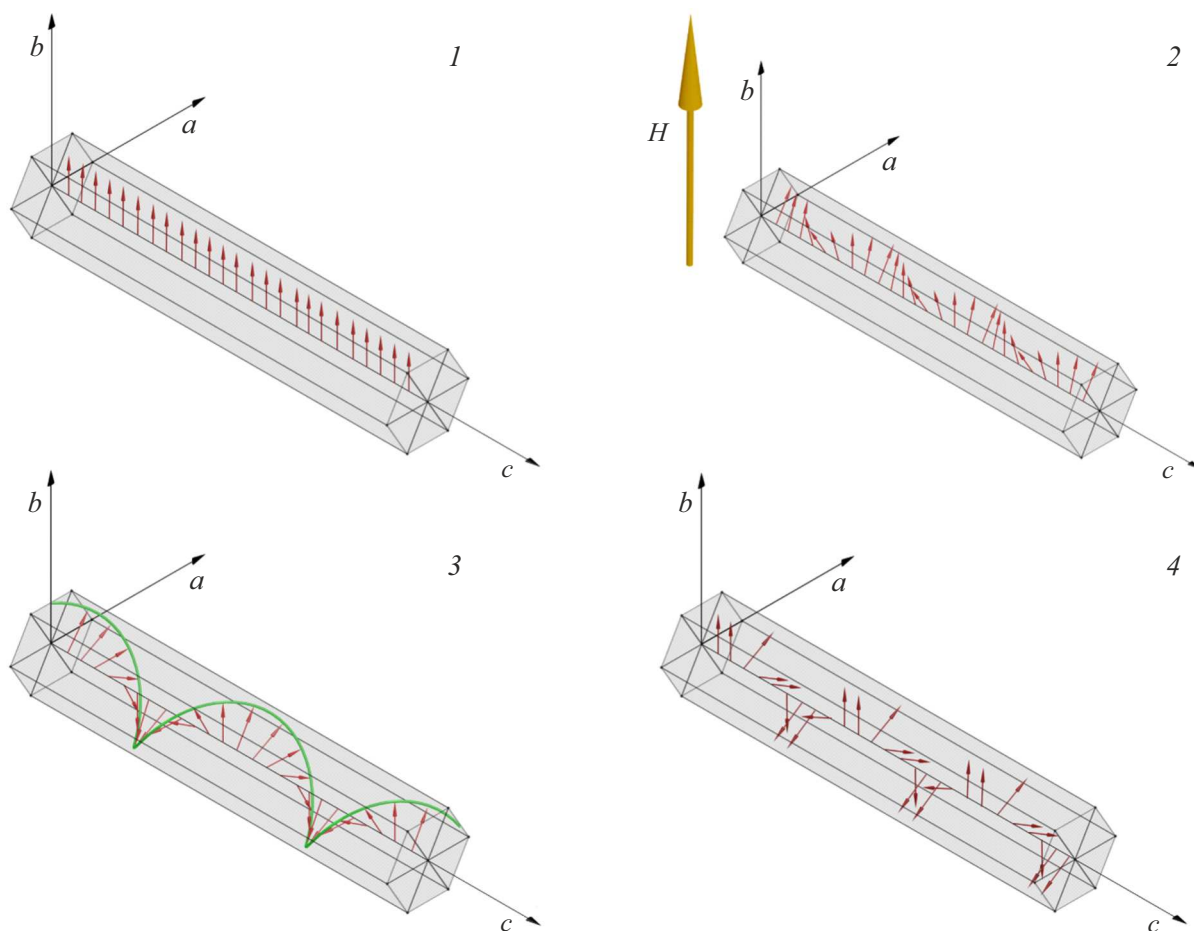


Figure 1. Ferromagnetic (1), fan (2), helix (3) and spin-slip (4) spin states in holmium films. The arrow shows the field direction.

The objective of this study was to determine critical indices of the ferro — helix, fan — helix, spin-slip — helix transitions and to analyze their values to obtain the

Table 1. Theoretical values of critical coefficients for various spin ordering models with different contribution ratios of x, y, z spin components

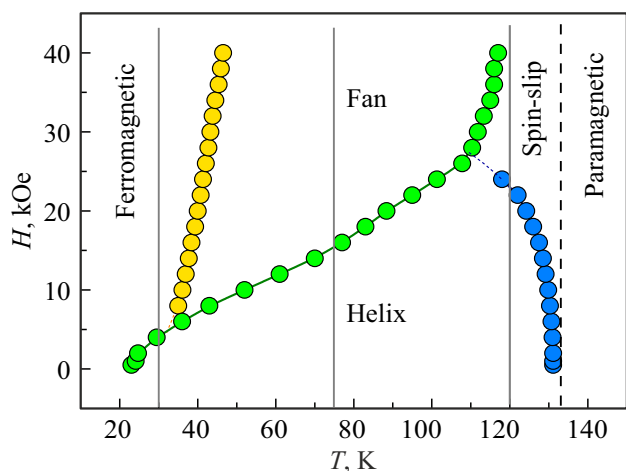


Figure 2. Magnetic phase diagram of the holmium film obtained by the SQUID magnetometer method in [2]. Vertical lines show the phase transition temperatures investigated by the Arrott plot method.

Applicable model	Critical coefficients β, γ	Reference
Mean-field	$\beta = 0.5$ $\gamma = 1$	[7]
Tricritical model	$\beta = 0.25$ $\gamma = 1$	[8]
3D-XY	$\beta = 0.346$ $\gamma = 1.316$	[7]
2D-Ising	$\beta = 0.125$ $\gamma = 1.75$	[9]
3D-Ising	$\beta = 0.325$ $\gamma = 1.24$	[7]
Heisenberg	$\beta = 0.365$ $\gamma = 1.386$	[7]

information on the exchange interaction models applicable to the description of noncollinear states of holmium films.

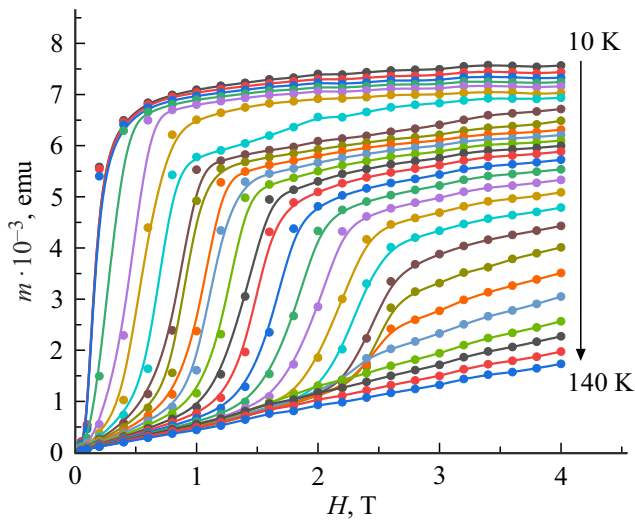


Figure 3. Field dependences of magnetic moment of Ho film obtained in the temperature range 10–140 K in increments of 5 K.

2. Procedure and samples

We used the magnetron sputtering method to deposit the 400 nm Ho film onto a MgO single-crystal substrate with an intermediate tungsten (W) buffer layer. W sputtering on MgO(100) first results in growth of W(100), that establishes the epitaxial growth in Ho with the c axis (0002) normal to the film. To protect the Ho film against oxidation, another 5 nm W layer was used. Before film deposition, the substrate was annealed at 800°C during 45 min, and then at 700°C during 30 min, then 10 nm W film was deposited at the same temperature. After that the sample was cooled to room temperature. Then the sample was coated with a 5 nm W layer. The 400 nm Ho film corresponds to ~ 60 periods of rotation of spin helix (each period is equal to 12 constants of 5.6 Å lattice on the c axis) within Ho.

Magnetic measurements were performed using SQUID MPMS XL Quantum Design magnetometer in the temperature range 10–140 K and magnetic field 0–4 T. Field dependences of magnetic moment m were measured at different temperatures measured in increments of 5 K (Figure 3). Further, the set of these curves was represented in $m^{1/\beta} ((H/m)^{1/\gamma})$ coordinates, while β and γ were selected such that $m^{1/\beta} ((H/m)^{1/\gamma})$ is a straight line at 30, 75, 120 K that were chosen by us to examine transitions from the helicoidal state to the ferro, helix, spin-slip configurations. Vertical lines in Figure 2 show the values of these temperatures and points of intersection with spin phase boundaries in various fields.

3. Experimental findings and discussion

Figure 3 shows isothermal field dependences recorded within 10–140 K. At high temperatures 135 and 140 K, linear dependences that characterize paramagnetic state of holmium are observed. Temperature decrease results

Table 2. Critical coefficients and transition temperatures measured by the Arrott method and possibly applicable models

Used model	Critical coefficients β, γ	Selected model	Phase transition temperature, K
Experimental coefficients	$\beta = 0.58$ $\gamma = 1.43$	Mean field	30
Experimental coefficients	$\beta = 0.35$ $\gamma = 1.34$	3D-XY	75
Experimental coefficients	$\beta = 0.43$ $\gamma = 1.30$	Heisenberg	120

in nonlinear dependences $m(H)$ indicating that magnetic-ordered spin states and phase transitions occur. Moreover, Figure 3 shows that there is a sharp bend in fields up to 3 T that suggests a transition induced by the magnetic field at a constant temperature. At low temperatures, transition to the ferromagnetic state and saturation of magnetization curves even in weak < 1 T fields are observed, and as the temperature grows, magnetization curves are far from saturation even in the 4 T field. Since the anisotropy constants grow in cooling, this suggests that temperature increase changes the magnetic phase to another one that has high anisotropy and saturation field.

For further analysis, this series of curves was represented in different coordinates so that selection of β and γ ensured rectification of curves at 30, 75, 120 K in $m^{1/\beta} ((H/m)^{1/\gamma})$ coordinates (Figure 4). Figure 4 shows curves in the Arrott coordinates for different critical coefficient values in the mean-field ($\beta = 0.5, \gamma = 1$) (Figure 4, a), tricritical mean-field ($\beta = 0.25, \gamma = 1$) (Figure 4, b), 3D-Ising ($\beta = 0.325, \gamma = 1.24$) (Figure 4, c), Heisenberg ($\beta = 0.365, \gamma = 1.368$) (Figure 4, d) models and for experimentally measured coefficients: ($\beta = 0.58, \gamma = 1.43$) for 30 K in transition from FM to Helix (Figure 4, e), ($\beta = 0.35, \gamma = 1.34$) for Helix–Fan transition at 75 K (Figure 4, f), ($\beta = 0.43, \gamma = 1.3$) for Helix–Spin-slip transition at 120 K (Figure 4, g). The Detail in Figure 4, g shows rectification at 120 K. Black solid lines show rectification of curve at the phase transition temperature.

For collinear ferromagnetic at $\beta = 0.5$ and $\gamma = 1$ in Figure 4, a, rectification of lines would have occurred in $m^2(H/m)$ coordinates in the mean-field model [10–12]. It is impossible to use the mean-field model for description of spin behavior within 10–140 K probably because the mean-field theory is not able to describe the helix or fan spin ordering in the system. Table 2 summarizes coefficients achieved by fitting the dependences at reference temperatures such that they become straight lines.

The measured dependences in Figure 4 suggest that the mean-field theory and tricritical models are not suitable for the Arrott plot analysis because the critical coefficients for these models do not provide rectification of curves at any phase transition temperature. The Ising and Heisenberg

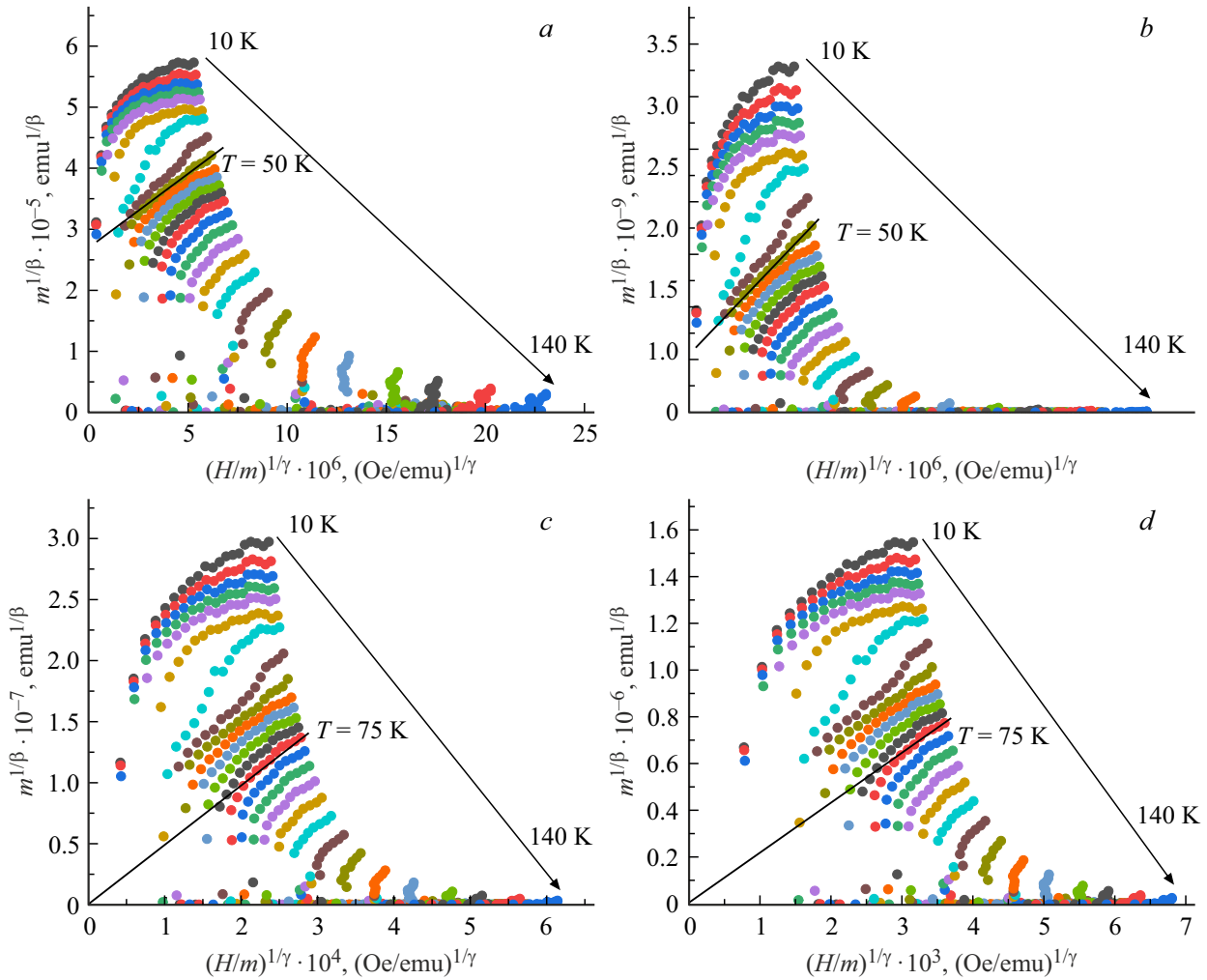


Figure 4. Arrott curves within 10–140 K in increments 5 K for Ho film. Critical coefficient correspond to the mean-field ($\beta = 0.5$, $\gamma = 1$) (a), tricritical mean-field ($\beta = 0.25$, $\gamma = 1$) (b), Ising ($\beta = 0.325$, $\gamma = 1.24$) (c), Heisenberg ($\beta = 0.365$, $\gamma = 1.368$) (d) models and experimental coefficients: ($\beta = 0.58$, $\gamma = 1.43$) for 30 K in transition from FM to Helix (e), ($\beta = 0.35$, $\gamma = 1.34$) for Helix–Fan transition at 75 K (f), ($\beta = 0.43$, $\gamma = 1.3$) for Helix–Spin-slip transition at 120 K (g). The Detail (g) shows rectification at 120 K. Black solid lines show rectification of curve at the phase transition temperature.

models make it possible to record transition from Helix to Fan spin states. Since the Arrott method was based on the Weiss mean-field theory, the Langevin function, that correlates magnetization with field and temperature, forms its basis

$$M = M_0 \tanh\left(\frac{\mu(H + NM)}{kT}\right). \quad (2)$$

Expression (2) may be written as expansion in series in M/M_0 :

$$\frac{\mu H}{kT} + N \frac{\mu M}{kT} = \frac{M}{M_0} + \frac{1}{3} \left(\frac{M}{M_0}\right)^3 + \frac{1}{5} \left(\frac{M}{M_0}\right)^5 + \dots \quad (3)$$

Equation (1) is derived from (3) by truncation of M/M_0 higher than third order. If the coefficients from Table 2 established by the Arrott analysis are compared with the theoretical coefficients from Table 1, transition between ferromagnetic and helicoidal states at 30 K with $\beta = 0.58$

and $\gamma = 1.43$ meets the „mean-field“ theory, though γ is a little overestimated. At 75 K in transition between helicoid and fan, $\beta = 0.35$ and $\gamma = 1.34$ closely match the 3D–XY-model. Finally, at 120 K, when transition from the helicoidal state to the spin-slip structure occurs, $\beta = 0.43$ and $\gamma = 1.3$, which is close to the Heisenberg model for three-dimensional spin ordering. In the latter case, the rectification of curves in $m^{1/\beta} ((H/m)^{1/\gamma})$ coordinates although is achieved, the corresponding straight line does not pass through the origin that may be explained by the fact that the terms higher than the third order in series in equation (3) cannot be truncated. This also may be the reason behind the overestimated γ for transitions at 30 and 120 K. All transitions analyzed herein are second-order transitions. Models with dominating exchange in the XY plane occur as a result of exchange interaction prevalence in the plane perpendicular to the c axis of the hexagonal structure [13]. It should be noted that critical indices are

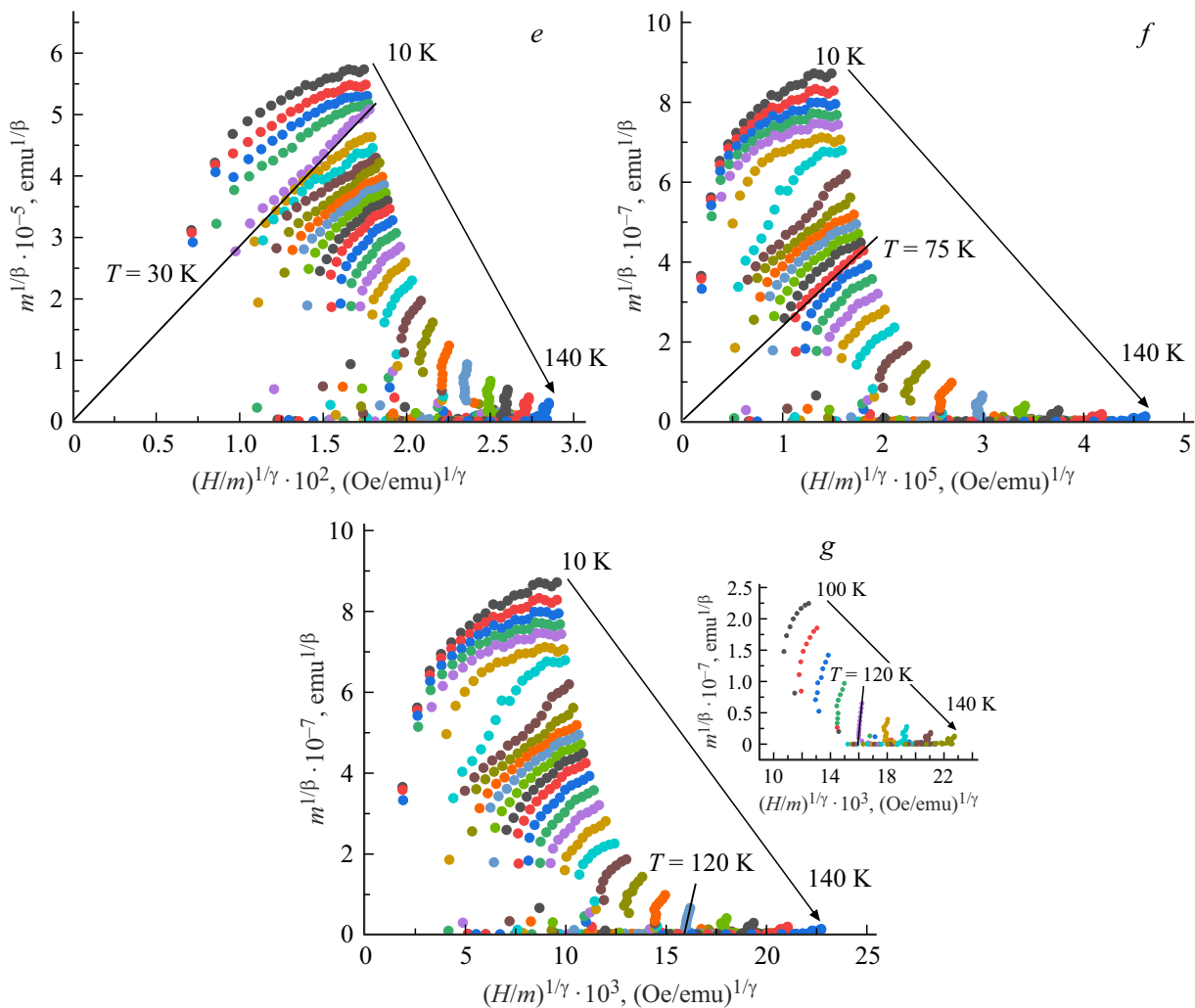


Figure 4 (continued).

generally connected with each other and, depending on dimension, relations that connect them may be of different kinds [12]. This study fails to determine simultaneously the dimension and all critical indices by determining these relations. However, the identified similarity of β and γ pairs with indices in known systems [7–9] suggests the equivalent universality classes for spin configurations in the examined holmium films.

4. Conclusion

In the holmium films whose properties are close to a bulk material, the Arrott plots were measured and the corresponding critical indices were defined to allow assertions about magnetic universality classes. The second-order transitions from the helicoidal state to ferromagnetic state are described by the „mean-field“ theory, transitions to the fan state are described by the 3D Ising model theory, and transitions to the spin-slip state are described by the standard Heisenberg model for the three-dimensional spin ordering. Thus, for several states to which holmium changes

from the helicoidal spin structure, universality classes are defined.

Funding

The study was carried out within the framework of thematic map 124013100858-3 of the Federal Research Center for Problems of Chemical Physics and Medical Chemistry of RAS.

Conflict of interest

The authors declare that they have no conflict of interest.

References

- [1] F.H.S. Sales, A.L. Dantas, A.S. Carriço. AIP Advances **2**, 3, 032158 (2012).
- [2] O. Koplak, R. Morgunov, R. Medapalli, E.E. Fullerton, S. Mangin. Phys. Rev. B **102**, 13, 134426 (2020).
- [3] J.R. Gebhardt, N. Ali. J. Appl. Phys. **83**, 11, 6299 (1998).

- [4] L.J. Rodrigues, V.D. Mello, D.H.A.L. Anselmo, M.S. Vasconcelos. *J. Magn. Magn. Mater.* **377**, 24 (2015).
- [5] J. Jensen. *J. Phys. Colloques* **49**, C8, C8-351 (1988).
- [6] I. Yeung, R.M. Roshko, G. Williams. *Phys. Rev. B* **34**, 5, 3456 (1986).
- [7] S.N. Kaul. *J. Magn. Magn. Mater.* **53**, 1–2, 5–53 (1985).
- [8] N. Moutis, I. Panagiotopoulos, M. Pissas, D. Niarchos. *Phys. Rev. B* **59**, 2, 1129 (1999).
- [9] Y. Wang, W. Liu, J. Zhao, J. Fan, L. Pi, L. Zhang, Y. Zhang. *New J. Phys.* **22**, 1 (2020).
- [10] M.E. Fisher. *The Nature of Critical Points*. University of Colorado Press (1965).
- [11] S. Ma. *Modern Theory of Critical Phenomena*. Routledge (1976).
- [12] B. Rosenstein, Yu Hoi-Lai, A. Kovner. *Phys. Lett. B* **314**, 3–4, 381 (1993).
- [13] S.T. Bramwell, P.C.W. Holdsworth. *J. Appl. Phys.* **73**, 10, 6096 (1993).

Translated by E.Ilinskaya